Single-Stage Quad-Active-Bridge Series-Resonant AC-DC Converter: Modulation for Active and Reactive Power

Daniel Chavez, Damian Sal y Rosas, Julio Tafur

Single-Stage Quad-Active-Bridge Series-Resonant AC-DC Converter: Modulation for Active and Reactive Power

Daniel Chavez[1,3]
[1]Universidad Nacional de Ingeniería
Lima, Peru
dachavezo@uni.pe

Damian Sal y Rosas[1,2]
[2]LAAS-CNRS, University of Toulouse,
31031 Toulouse, France
dsalyrosas@uni.edu.pe

Julio Tafur[3]
[3]Pontificia Universidad Católica del Perú
Lima, Peru
jtafur@pucp.edu.pe

2023 IEEE Energy Conversion Congress and Exposition (ECCE) | 979-8-3503-1644-5/23/$31.00 ©2023 IEEE | DOI: 10.1109/ECCE53617.2023.10362434

Abstract— **The single-stage AC-DC converters have a high potential to be used in electric vehicle (EV) chargers for vehicle-to-grid (V2G) applications due to its durability, high efficiency and reduced volume. In V2G applications, bidirectional active and reactive power transfer are required. However, reactive power transfer in single-stage AC-DC converters can increase considerably the high frequency (HF) current, reducing the converter efficiency. With the aim of overcoming this limitation, this article proposes a novel modulation for a single-stage three-phase AC-DC Quad-Active-Bridge Series-Resonant (QABSR) converter. The proposed modulation allows to obtain a HF current with a constant and minimum amplitude throughout grid period. Experimental results validate the converter steady-state response for bidirectional active and reactive power transfer.**

Keywords—«AC-DC converter», «Single-Stage», «Reactive Power», "bidirectional", «Quad-Active-Bridge», «series-resonant».

I. Introduction

The single-stage (SS) three-phase (3P) AC-DC converters allow bidirectional power flow and galvanic isolation, having better performances such as smaller volume, easier control, higher efficiency and longer lifetime compared to typical two-stage AC-DC converters [1]. Hence, SS 3P AC-DC converters have a high potential to be used in EV chargers with bidirectional active and reactive power transfer capability to implement V2G functionalities. Bidirectional active power transfer has been widely studied for SS AC-DC converters [1]. However, very few studies have been reported in the literature for bidirectional reactive power transfer using SS AC-DC converters.

For instance, the most popular SS 3P AC-DC converters are based on the Dual Active Bridge (DAB) converter [2], [3] which are shown in Fig. 1. The converter shown in Fig. 1a is composed of three independent single-phase (1P) SS AC-DC converters. A time-variant switching frequency and phase-shift (PS) modulation are used to control the bidirectional active power transfer. The converter drawbacks are the high number of switches used, having a high impact in converter efficiency and price, and the high complexity for implementing modulation and control strategy. Moreover, reactive power transfer has not been analyzed in these structures. The 3P DAB AC-DC converter shown in Fig. 1b [3] has fewer switches and components, increasing the converter efficiency and decreasing the price. However due to usage of bipolar voltage switches (in the matrix converter) to grid modulation, a complex modulation and switches protection have to be implemented. Modulation for reactive power transfer is proposed in [4] but its impact in the high frequency (HF) current has not been analyzed.

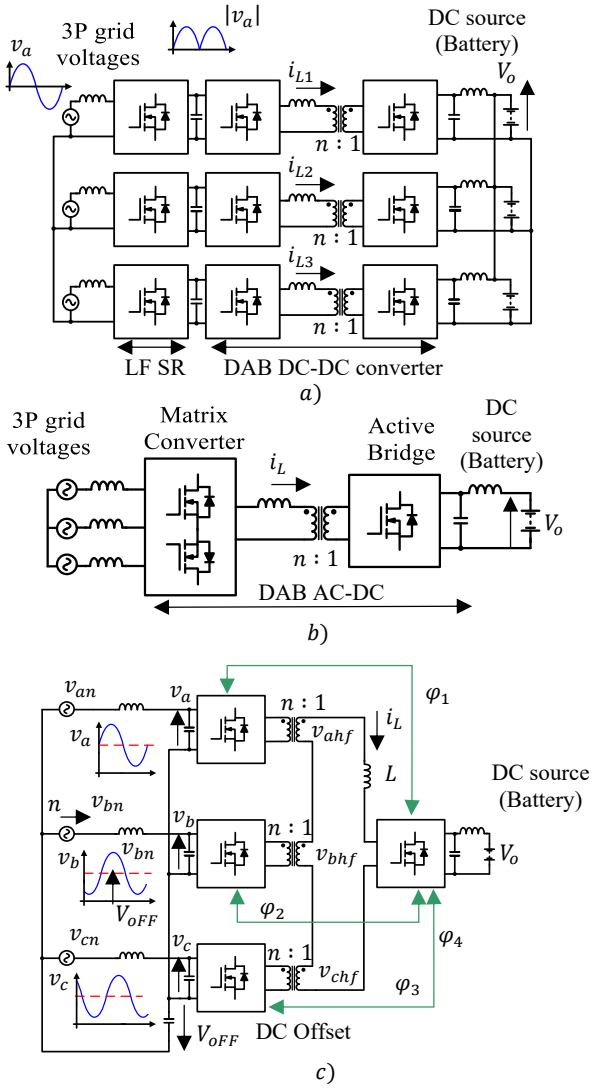

Fig. 1. Single-Stage 3P AC-DC DAB converters. a) Three 1P DAB AC-DC converters [2], b) 3P DAB AC-DC [3], c) 3P QAB AC-DC converter [5]

With the aim of avoiding the usage of bipolar voltage switches, the SS Quad-Active-Bridge (QAB) AC-DC converter shown in Fig. 1c was introduced in [5]. An offset is added in the grid voltages by means of controlling the DC voltage V_{oFF} in a series-connected capacitor to the grid neutral point (see Fig. 1c). Four PS angles ($\varphi_1, \varphi_2, \varphi_3$ and φ_4) are used to control the active power flow. However, the PS angles calculation and the control strategy are very complex to implement. Moreover, reactive power transfer has not been analyzed for this structure.

A deeper study for reactive power transfer using SS AC-DC converters with high MOSFETs quantity was reported in [6]. The authors shown that the HF current can be increased considerably for reactive power transfer which increases the converter losses. To overcome the drawbacks above mentioned, a novel modulation for a SS QAB series-resonant (QABSR) 3P AC-DC converter is proposed. A lower HF current is obtained compared to DAB or QAB AC-DC converters where a HF inductor is used [1]. The QABSR AC-DC converter implements duty ratio and PS modulations with an easier calculation, allowing the bidirectional active and reactive power control.

II. THE QABSR 3P AC-DC CONVERTER

The QABSR AC-DC converter is shown in Fig. 2. Three low-pass LC filters with a damping resistor r_d are used on the AC side. As in the QAB AC-DC converter, an offset V_{oFF} is controlled in capacitor C_f. Hence, the inputs on AC side are DC voltages with high ripple, allowing the usage of unipolar voltage switches to modulate the grid voltages. Moreover, three HF transformers are used which are series-connected on secondary side where a series-resonant circuit (SRC) is placed.

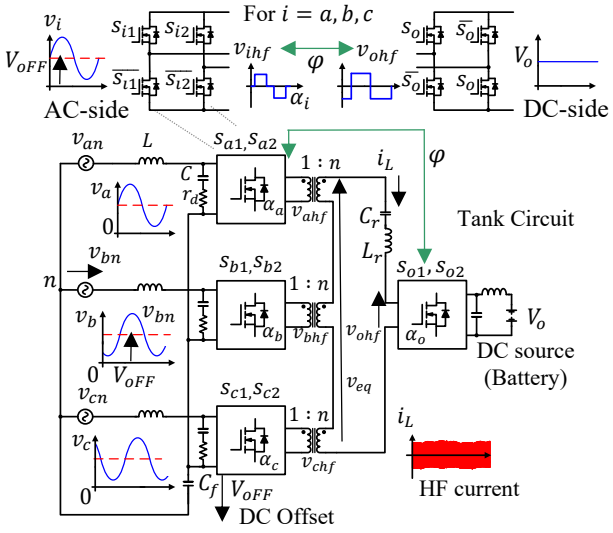

Fig. 2. Proposed QABSR 3P AC-DC converter.

Then, considering a balanced 3P system, the QAB inputs on AC side are given by:

$$v_i = V_{oFF} + v_{in} \;\; ; \;\; \text{for } i = a, b, c \tag{1}$$

Where:

$$\begin{cases} v_{an} = V_m \sin(\omega_g t) \\ v_{bn} = V_m \sin\left(\omega_g t - \frac{2\pi}{3}\right) \\ v_{cn} = V_m sin(\omega_g t + \frac{2\pi}{3}) \end{cases} \tag{2}$$

Whereas the grid currents are given by:

$$\begin{cases} i_a = I_m \sin(\omega_g t - \theta) \\ i_b = I_m \sin\left(\omega_g t - \frac{2\pi}{3} - \theta\right) \\ i_c = I_m sin(\omega_g t + \frac{2\pi}{3} - \theta) \end{cases} \tag{3}$$

Where V_m and ω_g the grid voltage amplitude and frequency respectively, I_m is the grid current amplitude whereas V_{oFF} is the DC offset voltage controlled in the capacitor C_f such that $V_{oFF} > V_m$ (see Fig. 2). Note in (3) that the angle θ allows to control the transfer of reactive power in the grid.

In the proposed modulation four duty ratio (DR) angles α_a, α_b, α_c and α_o and only one phase-shift (PS) angle φ are used as command signals, being the modulation functions given by:

AC side:

$$\begin{cases} s_{i1} = sgn\left(\cos\left(\omega_s t - \frac{\alpha_i}{2}\right)\right) \\ s_{i2} = sgn\left(\cos\left(\omega_s t + \frac{\alpha_i}{2}\right)\right) \end{cases} \text{for } i = a, b, c \tag{4}$$

DC side:

$$\begin{cases} s_{o1} = sgn\left(\cos\left(\omega_s t - \frac{\alpha_o}{2} - \varphi\right)\right) \\ s_{o2} = sgn\left(\cos\left(\omega_s t + \frac{\alpha_o}{2} - \varphi\right)\right) \end{cases} \tag{5}$$

Where ω_s is the switching frequency and the function $sgn(x)$ is defined as:

$$sgn(x) = \begin{cases} 1, & when \; x \geq 0 \\ 0, & when \; x < 0, \end{cases} \tag{6}$$

The modulated voltages v_{ahf}, v_{bhf}, v_{chf} and v_{ohf}, evaluated at $\omega_g t = \frac{3\pi}{10}$ are shown in Fig. 3.

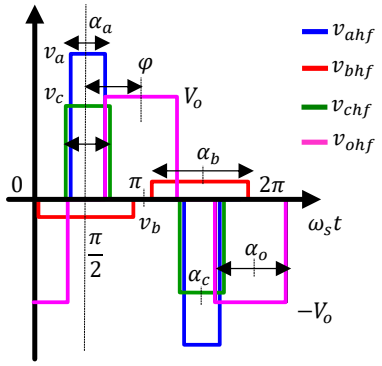

Fig. 3. Proposed modulation for the QABSR 3P AC-DC converter

Note that the DR angles α_a, α_b and α_c are used to modulate the input voltages v_a, v_b and v_c respectively given by (1), generating the HF voltages v_{ahf}, v_{bhf} and v_{chf}. Whereas, the DC source V_o is modulated by the DR angle α_o generating the HF voltage v_{ohf} which is phase-shifted φ with respect to v_{ahf}, v_{bhf} and v_{chf}, as shown in Fig. 2 and Fig. 3.

On the other hand, the tank circuit is designed as a band-pass filter at switching frequency ω_s [6]. Hence, only the components at ω_s are considered for power transfer, it means:

For the modulated DC Source:

$$v_{ohf1} = \frac{4}{\pi} V_o \sin\left(\frac{\alpha_o}{2}\right) \sin(\omega_s t - \varphi); \quad (7)$$

Whereas, for the modulated grid voltages with OFFSET:

$$v_{ihf1} = \frac{4}{\pi} V_{ihf1} \sin(\omega_s t); \quad (8)$$

Where:

$$V_{ihf1} = v_i \sin\left(\frac{\alpha_i}{2}\right); \text{ For } i = a, b, c \quad (9)$$

Being $v_i = V_{OFF} + v_{in}$ defined in (1) whereas $\frac{\alpha_i}{2}$ is the correspondent DR angle $\frac{\alpha_a}{2}$, $\frac{\alpha_b}{2}$ and $\frac{\alpha_c}{2}$ respectively. In the proposed modulation $\frac{\alpha_a}{2}$, $\frac{\alpha_b}{2}$ and $\frac{\alpha_c}{2}$ take the instantaneous values of the grid current angles given by (3), it means:

$$\begin{cases} \frac{\alpha_a}{2} = \omega_g t - \theta; \\ \frac{\alpha_b}{2} = \omega_g t - \frac{2\pi}{3} - \theta; \\ \frac{\alpha_c}{2} = \omega_g t + \frac{2\pi}{3} - \theta; \end{cases} \quad \text{Where } \omega_g t \in [0; 2\pi] \quad (10)$$

Hence, V_{ihf1} given by (9) can be considered constant during one switching period because $\omega_s \gg 2\omega_g$. The series-connection of the HF transformers, on the secondary side, allows to add the modulated voltages v_{ahf}, v_{bhf} and v_{chf} given by (8), resulting:

$$v_{eq1} = \frac{4}{\pi} n \left[v_a \sin\left(\frac{\alpha_a}{2}\right) + v_b \sin\left(\frac{\alpha_b}{2}\right) + v_c \sin\left(\frac{\alpha_c}{2}\right) \right] \sin(\omega_s t) \quad (11)$$

Hence, replacing (2) and (10) in (11):

$$v_{eq1} = \frac{4}{\pi} n \left[\frac{3}{2} V_m \cos(\theta) \right] \sin(\omega_s t) \quad (12)$$

Where V_m is the grid voltages amplitude and n is the turns-ratio relationship of HF transformers. According to (12) the voltage v_{eq1}, on the secondary side of HF transformers (see Fig.2), has a constant amplitude $\frac{4}{\pi} n \left[\frac{3}{2} V_m \cos(\theta) \right]$ throughout the grid period. For instance, the modulated voltages v_{ahf}, v_{bhf} and v_{chf} as well as the voltage on the HF transformers secondary side $v_{eq} = v_{ahf} + v_{bhf} + v_{chf}$ (see Fig.2) for $\theta = 0°$ and evaluated at $\omega_g t = \frac{\pi}{2}$ are shown in Fig. 4.

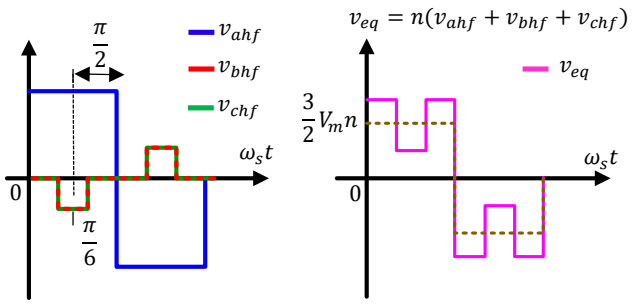

Fig. 4. The modulated voltages evaluated at $\theta = 0$ and $\omega_g t = \frac{\pi}{2}$

Note that v_{eq} can reach high voltage peaks where the highest can be obtained by deriving v_{eq}, having its maximum value at $\omega_g t = \frac{\pi}{6}$.

On the other hand, for power transfer, only the switching frequency component v_{eq1} given by (12) is considered, which is decreased by the power factor $\cos(\theta)$. Hence, for high reactive power transfer $\theta \to \frac{\pi}{2}$, $\cos(\theta) \to 0$ and $v_{eq1} \to 0$ which can increase considerably the HF current amplitude [6]. With the aim of compensating the voltage drop in v_{eq1} for high reactive power transfer, the DC source is modulated with the DR angle α_o according to the following relationship:

$$\frac{\alpha_o}{2} = \frac{\pi}{2} - |\theta| \quad (13)$$

Hence v_{eq1} and v_{ohf1} amplitudes can be controlled to have a constant value amplitude throughout grid period. With this consideration, the tank circuit along with the turns-ratio n can be sized, considering the maximum values of v_{eq1} and $v_{ohf1}(\theta = 0)$, it means as an equivalent DABSR DC-DC converter for two DC sources: $\frac{3}{2} V_m$ and V_o [6], [7]. Then, n and the SRC can be sized as follows:

$$n = \frac{V_o}{\frac{3}{2} V_m}; \quad Q = \frac{Z}{\frac{8}{\pi^2} R_o}; \quad \omega_r = \frac{1}{\sqrt{L_r C_r}}; \quad Z = \sqrt{\frac{L_r}{C_r}}; \quad F = \frac{\omega_s}{\omega_r}; \quad R_o = \frac{{V_o}^2}{P_o} \quad (14)$$

Being L_r and C_r the inductance and capacitance of the SRC, Q and ω_r the quality factor and resonance frequency of the SRC, P_o the nominal power and R_o the nominal output load.

Then, the average input currents $\langle i_a \rangle$, $\langle i_b \rangle$ and $\langle i_c \rangle$, for one switching period, can be calculated as:

$$\begin{cases} \langle i_a \rangle = [K \sin(\varphi)] \sin\left(\frac{\alpha_a}{2}\right); \\ \langle i_b \rangle = [K \sin(\varphi)] \sin\left(\frac{\alpha_b}{2}\right); \\ \langle i_c \rangle = [K \sin(\varphi)] \sin\left(\frac{\alpha_c}{2}\right); \end{cases} \quad (15)$$

Where:

$$K = \frac{8nV_o \sin(\frac{\alpha_o}{2})}{\pi^2 Z \left(F - \frac{1}{F}\right)} \quad (16)$$

Being the DR angles $\frac{\alpha_a}{2}, \frac{\alpha_b}{2}, \frac{\alpha_c}{2}$ given by (10). Note in (15) that, the factor $K \sin(\varphi)$ is repeated in the three average currents whereas, each average current depends on its respectively DR angle. Hence the DR angles control the shape of the grid currents whereas φ controls the grid current amplitude. Hence, comparing (3) with (15), the PS angle φ can be calculated as:

$$\varphi = asin\left(\frac{I_m}{K}\right) \quad (17)$$

Where K is defined in (16). Note that, with the proposed modulation, a decoupled control can be implemented for each grid current, using the DR angles $\frac{\alpha_a}{2}, \frac{\alpha_b}{2}, \frac{\alpha_c}{2}$ as a control signals and φ taking a constant value throughout the grid period, making the proposed modulation and control easier to implement.

III. Experimental Results

The proposed converter was validated using the parameters indicated in Table I.

TABLE I. QABSR AC-DC Converter Parameters

Item	Value	Item	Value
Output voltage and power (V_o, P_o)	400V, 2 kW	Tank circuit (L_r, C_r)	380 μH, 5.5 ηF
Grid Voltage (line - neutral)	220V RMS, 60 Hz	Turns-ratio relationship (1: n)	1: 0.86
Switching frequency (f_s)	120 kHz	Tank circuit parameters (F, Q)	$F = 1.1$ $Q = 4$
OFFSET V_{oFF} and C_f	350V, 4.7μF	LC Input Filter (L_i, C_i, r_d)	200μH, 1μF, 1.1Ω

Note that the series-connected capacitor C_f in grid neutral point takes a small capacitance value ($C_f = 4.7\mu F$) unlike a DC-link capacitor used in two-stage AC-DC converters which can take mF values [8]. Moreover, $V_{oFF} = 350V > V_m = 220\sqrt{2} = 311.12V$. Whereas, the LC AC filters take a small inductance value compared to two-stage AC-DC converters [6].

The experimental setup is shown in Fig. 5. With the aim of validating the bidirectional power flow, a three-phase (3Ø) AC source were used. Similarly, a bidirectional DC source was used on the DC side.

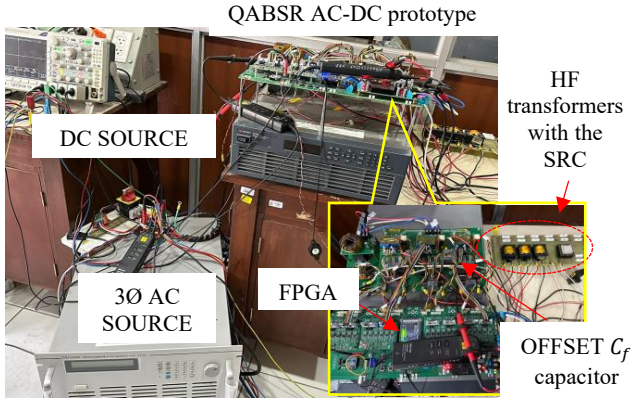

Fig. 5. The experimental setup for the QABSR AC-DC 2 kW prototype

First, the controlled DC voltage V_{OFF} in the grid neutral point was validated. The grid voltage v_{an}, the grid voltages with offset $v_a = v_{an} + V_{oFF}$, v_b, v_c andV_{OFF} are shown in Fig. 6. The DC voltage V_{OFF} is controlled to $\approx 350V$.

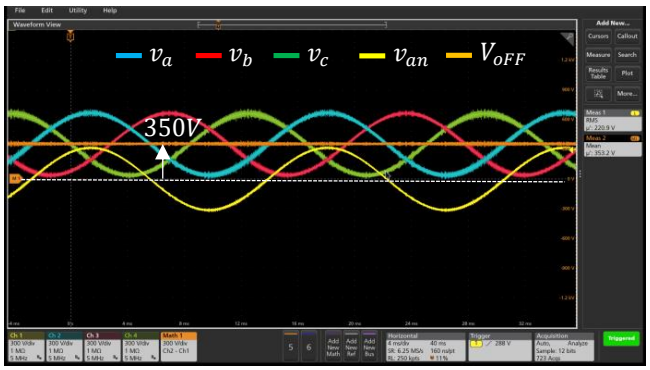

Fig. 6. QABSR input voltages v_a, v_b and v_c with a DC offset.

The 3Ø grid currents for grid-to-vehicle (G2V) and vehicle-to-grid (V2G) modes are shown in Fig. 7 and 8 respectively, considering $\theta = 30°$ (active and reactive power transfer).

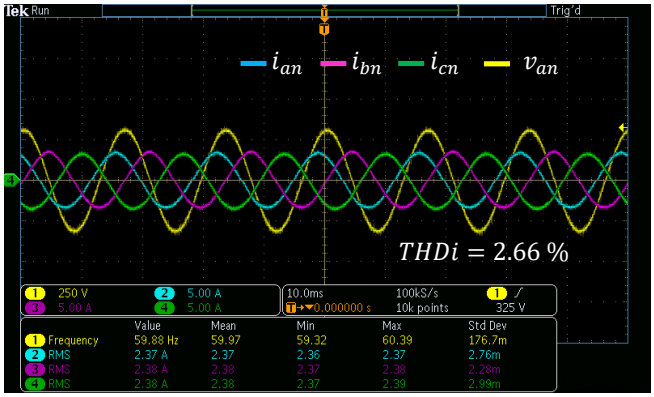

Fig. 7. Grid currents for G2V considering active and reactive power ($\theta = 30°$)

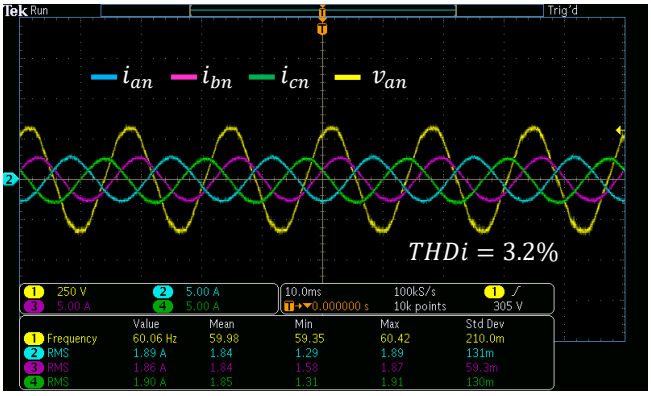

Fig. 8. Grid currents for V2G considering active and reactive power ($\theta = 30°$)

Note that, for G2V the THD is lower than V2G mode. This result is obtained because for V2G test, the converter was directly connected to the grid voltages which present some low frequency harmonics unlike the 3Ø source as shown in Fig.7.

In Fig. 9 and 10 are shown the grid current i_{an}, the DC output current i_o, and grid voltage v_a for inductive ($\theta = 30°$) and capacitive ($\theta = -30°$) reactive power in G2V, respectively.

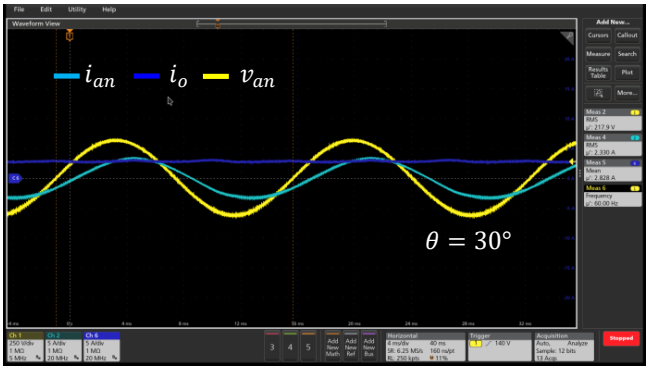

Fig. 9. Reactive power G2V for $\theta = 30°$ and $\frac{\alpha_o}{2} = 60°$

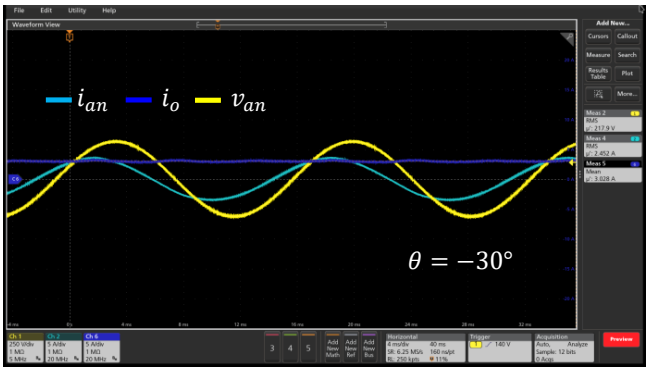

Fig. 10. Reactive power G2V for $\theta = -30°$ and $\frac{\alpha_o}{2} = 60°$

The modulated grid voltages v_{ahf} and v_{ohf} along with the HF current evaluated at $\frac{\alpha_a}{2} = \frac{\pi}{2}$ and $\frac{\alpha_o}{2} = \frac{\pi}{3}$ for G2V mode is shown in Fig. 11. Note that ZVS mode is obtained for both active bridges (ABs). Hence high efficiency is achieved.

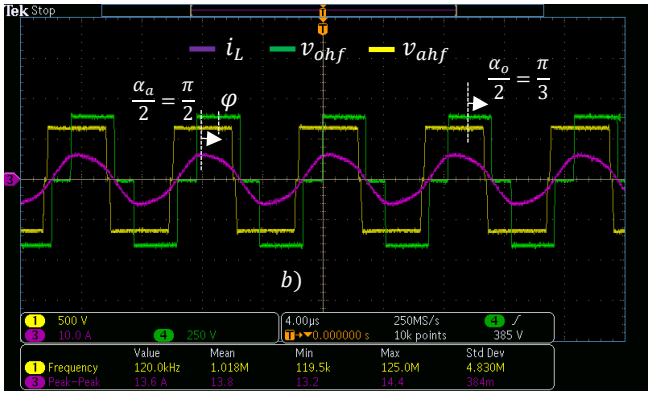

Fig. 11. Modulated grid voltages and HF current for G2V at $\omega_g t = \frac{\pi}{2}$

Likewise, the grid current i_{an} for inductive ($\theta = 30°$) and capacitive ($\theta = -30°$) and V2G mode are shown in Fig. 12 and 13 respectively. Therefore, bidirectional active and reactive power flow was validated for V2G and G2V mode implementing the proposed modulation.

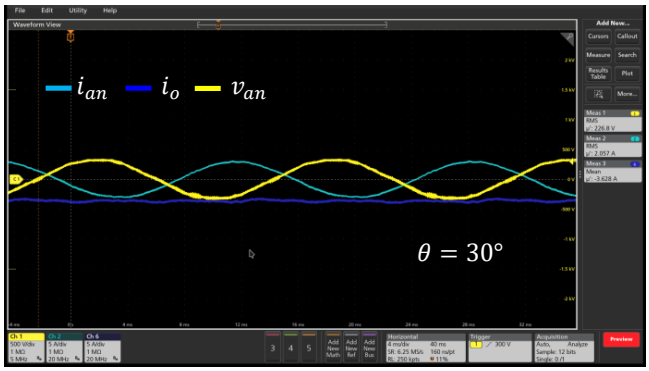

Fig. 12. Reactive power V2G for $\theta = 30°$ and $\frac{\alpha_o}{2} = 60°$

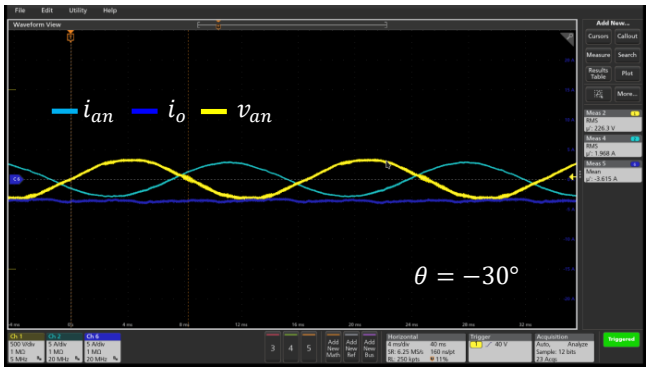

Fig. 13. Reactive power V2G for $\theta = -30°$ and $\frac{\alpha_o}{2} = 60°$

The modulated grid voltages and HF current for V2G mode (evaluated at $\frac{\alpha_a}{2} = \frac{2\pi}{5}$ and $\frac{\alpha_o}{2} = \frac{\pi}{3}$) are shown in Fig. 14. Note that ZVS mode is obtained for both ABs. Moreover, the measured efficiency in G2V was lower than V2G mode (95.4% vs 96.2%). This decrease in the efficiency is because ZVS mode

is lost in one leg of the ABs, on the AC side, for G2V when the DR angles $\alpha_a, \alpha_b, \alpha_c$ take small angle values.

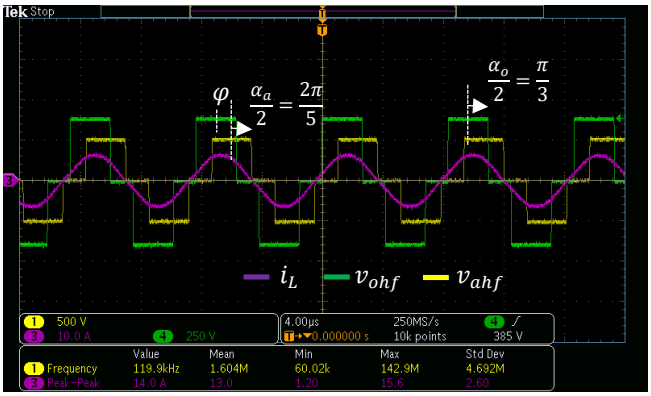

Fig. 14. Modulated grid voltages and HF current for V2G for $\omega_g t = \frac{2\pi}{5}$

Finally, the HF 3P power decoupling is validated in Fig. 15 where the modulated voltages v_{ahf}, v_{bhf}, v_{chf} and the HF current i_L are shown for three grid periods. Note that the HF current has a constant amplitude throughout the grid period.

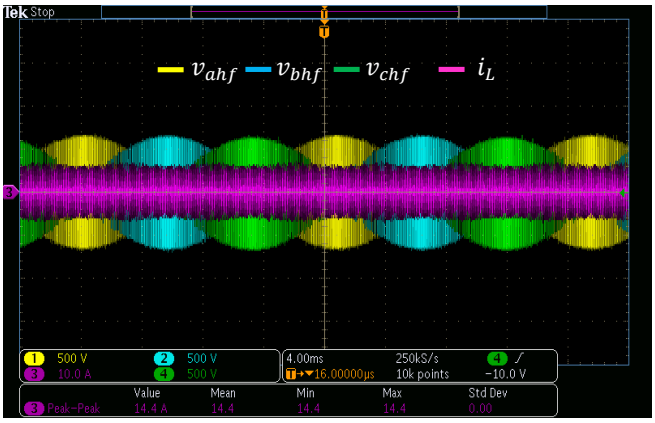

Fig. 15. Modulated grid voltages and HF current in the tank circuit for three grid periods.

The efficiency analysis for G2V is shown in Fig. 16.

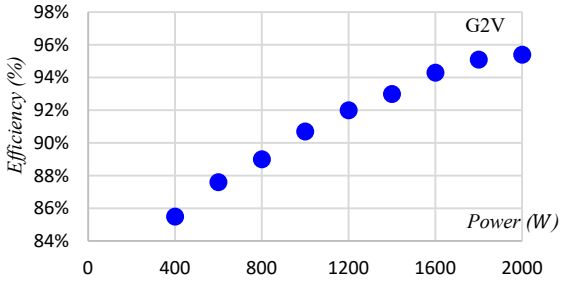

Fig. 16. Efficiency analysis for G2V mode.

Note that the highest efficiency is obtained in G2V mode for the nominal power. In contrast, the lowest efficiency is obtained for the lower power transfer.

IV. Conclusions

A novel modulation for the single-stage QABSR 3P AC-DC converter is proposed in this article. The grid voltages with the DC offset are modulated by duty ratio modulation whereas the DC source is modulated by duty ratio and phase-shift modulation. The duty ratio and phase-shift angles can be easily calculated. The proposed modulation has the following advantages: (1) to control the bidirectional active and reactive power transfer with a decoupled grid currents control, (2) to obtain a HF current with a constant and smaller amplitude value throughout the grid period compared with other single-stage AC-DC structures, (3) ZVS mode is achieved in all active bridges obtaining high efficiency. Hence, the QABSR AC-DC converter implementing the proposed modulation is a good candidate for EV chargers implementing V2G functionalities. Futures studies will be focused in the analysis of closed-loop control with unbalanced grid voltages and improved dynamic response.

Acknowledgment

This wok was financed by CONCYTEC-PROCIENCIA by the project “Manufactura Avanzada de Estaciones de recarga rápida de vehículos eléctricos basada en Sistemas Fotovoltaicos Inteligentes” [Contract N° 007-2021].

References

[1] F. Wu, K. Wang, G. Hu, Y. Shen and S. Luo, “Overview of Single-Stage High-Frequency Isolated AC–DC Converters and Modulation Strategies”, IEEE Trans. on power electronics, Vol. 38, no. 2, Feb. 2023

[2] J. Lu, K. Bai, A. R. Taylor, G. Liu, A. Brown, P. Johnson and M. McAmmond, “A Modular-Designed Three-Phase High-Efficiency High-Power-Density EV Battery Charger Using Dual/Triple-Phase-Shift Control”, IEEE Trans. on power electronics, Vol. 33, no. 9, Sep. 2018

[3] L. Schrittwieser, M. Leibl and J. W. Kolar. “99% Efficient Isolated Three-Phase Matrix-Type DAB Buck–Boost PFC Rectifier”, IEEE Trans. on power electronics, Vol. 35, no.1, Jan. 2020

[4] Koji Shigeuchi, Jin Xu, Noboru Shimosato and Yukihiko Sato, “A Modulation Method to Realize Sinusoidal Line Current for Bidirectional Isolated Three-Phase AC/DC Dual-Active-Bridge Converter Based on Matrix Converter”, IEEE TRANS. ON POWER ELECTRONICS, VOL. 36, NO. 5, pp. 6015-6029, MAY 2021

[5] B. Vermulst, J. L. Duarte, C. G. E. Wijnands and E. Lomonova, “Quad-Active-Bridge Single-Stage Bidirectional Three-Phase AC–DC Converter with Isolation: Introduction and Optimized Modulation”, IEEE Trans. on power electronics, Vol. 32, no. 4, pp. 2546-2557, April 2017.

[6] D. Sal y Rosas, D. Chavez, D. Frey, JP. Ferrieux, “Single-Stage Isolated and Bidirectional Three-Phase Series-Resonant AC-DC Converter: Modulation for Active and Reactive Power Control”, in Energies Journal, Oct. 2022.

[7] Damian Sal y Rosas, David Frey, Jean-Paul Ferrieux, “Isolated single stage bidirectional AC-DC converter with power decoupling and reactive power control to interface battery with the single-phase grid”, in Proc. of APEC, Mars 2018.

[8] Damian Sal y Rosas, Alvaro Zarate, “Single-Phase Grid-Forming Strategy with Power Decoupling Implementation for Electrolytic-Capacitor-Free EV Smart Battery Charger”, in Energies Open Access Journal, 16(2), 894; https://doi.org/10.3390/en16020894, JAN. 2023